

NUMERICAL STUDY OF THE PERFORMANCE IMPROVEMENT OF SUBMERGED AIR INTAKES USING VORTEX GENERATORS

César Celis Pérez*, Sandro Barros Ferreira*, Luís Fernando Figueira da Silva*, Antonio Batista de Jesus, Guilherme Lara Oliveira****

***Pontificia Universidade Católica do Rio de Janeiro - BRAZIL, **Empresa Brasileira de Aeronáutica SA - EMBRAER - BRAZIL**

Keywords: air intake, transport aircraft, vortex generator

Abstract

In this paper the results of a computational investigation related to the performance improvement of submerged air intakes using vortex generators are presented. A delta wing vortex generator is designed and assembled to a conventional NACA inlet. Then, parametric variations of the vortex generator geometry are performed. The results show that the inclusion of the vortex generator is responsible for considerable reductions of the boundary layer thickness and, consequently, significant improvements of the performance parameters of the NACA inlet. The obtained improvements, in terms of ram recovery ratio and mass flow rate, are of up to 57.5% and 20.5%, respectively. The contribution of the drag induced by the presence of the vortex generator on the total drag of the ensemble is small, about 10%.

1 Introduction

NACA intakes, Fig. 1, have been widely used in aircraft as a low drag source of external flow for air conditioning, ventilation and cooling systems. The design criteria of these intakes have been established during the 1940's and 50's. Recently, classical aircraft intakes have been revisited with the use of Computational Fluid Dynamic techniques (CFD), aiming to improve their performance. These performance improvements have been sought with the use of the following techniques: (i) vortex generators [1, 2] (ii) flow deflectors [3, 4], (iii) parametric

geometric optimization [5], and (iv) pulsating jets [6].



Fig. 1. Conventional NACA inlet [1].

The literature [2, 3, 7] indicates that the boundary layer thickness upstream of the air intake is the key parameter governing the performance of this type of inlets, and that the larger the boundary layer thickness, the poorer the performance of the air inlet. In particular, Ref. [2] shows that the introduction of a pair of vane type vortex, upstream of the air inlet, resulted in a thinning of the boundary layer thickness and, consequently, in a 34% increase of the ram recovery ratio of the air intake. So, in this work, it is examined the use of a vortex generator type delta wing in order to reduce the boundary layer thickness, and to enhance the performance of a conventional NACA intake.

Delta wings are usually employed in supersonic airplanes, because they induce low wave drag while yielding high values of lift coefficient. These high values of lift coefficient are associated to the high levels of vorticity produced by the vortex generated along the suction side of the delta wing. Those vortices

increase the lift and energize the boundary layer over the wing, so that the stall angle can be increased. In this work, the vortex generated by the delta wing will be shown to reduce the boundary layer thickness through the mixing of high momentum air from the free-stream flow with the low energy boundary layer air, in order to increase the performance of the NACA intake.

The goal of this work is to evaluate the influence of the use of delta wing vortex generators on the development of the boundary layer upstream of the NACA inlet. Three parametric variations of the vortex generator geometry are studied: horizontal positioning, angle of attack and area of the vortex generator. The results of these parametric variations are analyzed both qualitatively and quantitatively.

2 Numerical Approach

2.1 Description of the geometric configurations

In this numerical study are simulated and analyzed three configurations. The conventional NACA intake, which geometric characteristics are shown in Fig. 2, is the first configuration studied in this work. This configuration corresponds to a typical one used in a regional transport aircraft. The flow conditions analyzed correspond to a Mach number of 0.31, an altitude of 9,000 ft and a temperature of -2.83°C . The results of this configuration will be used as a reference to evaluate the performance of the NACA intake when the vortex generator is utilized.

The configuration of the vortex generator type delta wing and the configuration resulting from the assembly of the conventional NACA inlet to the vortex generator constitute the other two configurations studied in this work. The results of the simulations of the configuration corresponding to the vortex generator will not be shown here, but it is important to highlight that these results were used to define the position of the vortex generator with respect to the NACA intake.

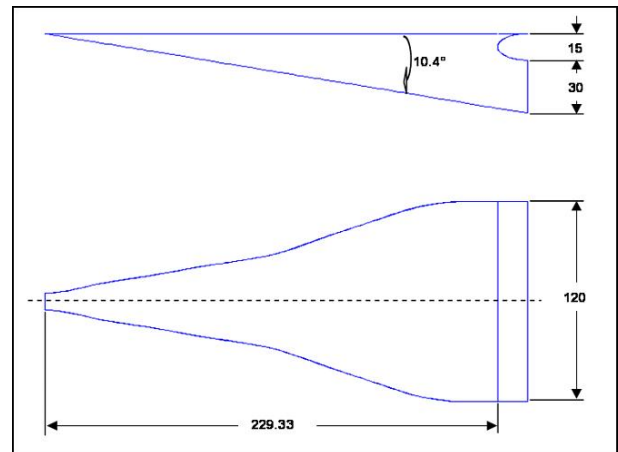


Fig. 2. NACA air inlet geometry (dimensions in mm).

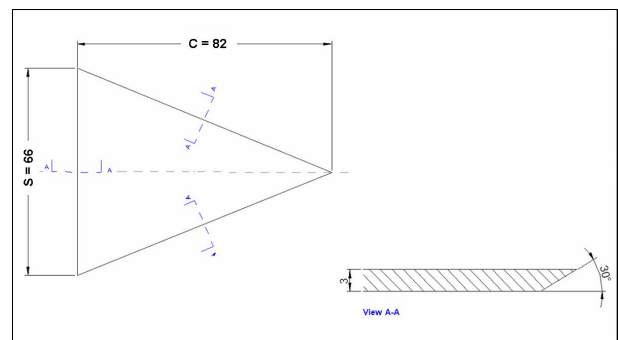


Fig. 3. Vortex generator geometry (dimensions in mm).

2.2 Mesh generation

Grid generation of the studied configurations was performed using the commercial software ANSYS ICEM CFD, Version 5.0 [8]. In the case of the conventional NACA intake, the computational domain consisted of a NACA inlet placed at the center of a flat plate of $10,000 \times 2,000 \text{ mm}^2$, a duct of rectangular cross section coupled to the NACA inlet throat, and a parallelepiped of $10,000 \times 1,000 \times 1,000 \text{ mm}^3$ as farfield. The NACA inlet was placed at 5,000 mm from the beginning of the domain. For the cases of NACA inlet with vortex generator, additionally, the vortex generator is placed upstream of NACA intake. Symmetry is assumed at the central plane of the inlet and of the vortex generator.

All the meshes used in this work, one of which is shown in Fig. 4, were structured meshes composed by hexahedral elements. The mesh of the conventional NACA intake was

composed of about 255,000 elements, and the number of elements of the meshes corresponding to the configurations of NACA inlet with vortex generator consisted of nearly 1,100,000 elements.

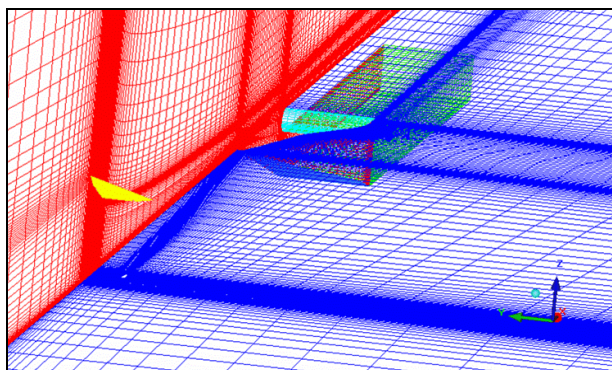


Fig. 4. Shell mesh of a generic configuration of NACA inlet and vortex generator.

2.3 Flow solver

All the numerical simulations were conducted using the commercial CFD package FLUENT, Version 6.1 [9]. For the resolution of the governing equations of the compressible flow, *Fluent* uses a control-volume-based technique, which consists of the division of the domain into discrete control volumes using a computational grid. The integration of the governing equations on the individual control volumes allows to construct algebraic equations for the discrete dependent variables. The linearization of the discretized equations and solution of the resultant linear equation system yields updated values of the dependent variables.

In this work, an implicit segregated solver was used to solve the governing equations along with a Spalart-Allmaras [10] turbulence model. The interpolation scheme used for the convection term was the Second-Order Upwind Scheme, and the Second-Order for calculating face Pressure. The algorithm applied for Pressure-Velocity Coupling was SIMPLE (*Semi-Implicit Method for Pressure-Linked Equations*) [9].

2.4 Boundary and Initial conditions

Fig. 5 illustrates the computational domain where the boundary conditions were set. At the farfield, zone 1, free-stream conditions with a given Mach number, static pressure and temperature were specified. At the duct exit section, zone 2, a constant static pressure was specified. No-slip adiabatic boundary conditions were set at the solid walls, zone 3. Finally, symmetry conditions were set at the symmetry plane of both the conventional NACA intake and the vortex generator.

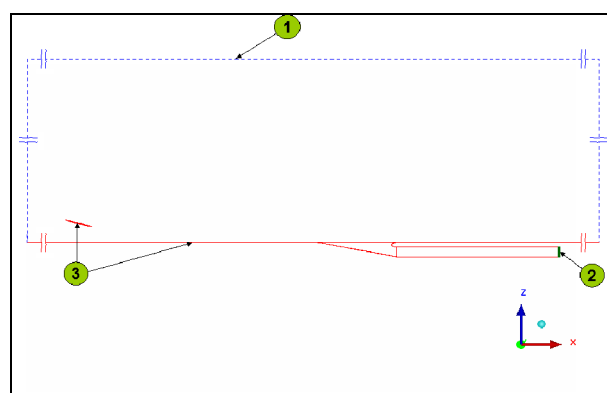


Fig. 5. NACA inlet with vortex generator – Symmetry plane.

The computations were initialized from free-stream conditions given in Table 1.

Table 1. Free-stream conditions.

Pressure (p)	(Pa)	72,428
Temperature (T)	(K)	270.3
Mach number (M)	-----	0.31
Modified Turbulent Viscosity ($\tilde{\nu}$)	(m^2/s)	0.001

3 Results and Discussion

Table 2 summarizes the different configurations studied in this work. In this table, HD represents the horizontal distance between the trailing edge of the vortex generator and the beginning of the ramp of the NACA inlet, and α is the angle of attack of the vortex generator. The area of the basic vortex generator is $A = 2,706 \text{ mm}^2$. The vertical distance between the trailing edge of the vortex generator and the flat plate, in all the configurations tested, was 50 mm. For the sake of simplicity, the results which will be shown

here will be referenced to their respective codes indicated in Table 2.

Table 2. Summary of the configurations simulated.

Case	HD (mm)	α (°)	Area of VG
N1A-1	DATUM		
NGVA	700	15	A
NGVB	500	15	A
NGVC	300	15	A
NGVA-25	700	25	A
NGVA-35	700	35	A
NGVA-1.5A	700	15	1.5A
NGVA-2.0A	700	15	2.0A

Regarding the convergence criterion of the simulated cases in this work, it is important to emphasize that, in all the computations performed here, the solver execution was interrupted only after the residuals of all the computed variables achieved their complete stabilization.

3.1 Conventional NACA intake

It is well known that the boundary layer thickness is a determinant parameter of the efficiency of a NACA inlet. So, in order to understand the influence of the vortex generator upon the boundary layer, plots describing the boundary layer development upstream to the NACA inlet will be analyzed. Moreover, since the inlet efficiency is computed based on the throat flow, the distribution of the pressure coefficient along the throat plane of the NACA intake is also shown. Fig. 6 shows cross sections, in transversal planes to the external flow direction, of the longitudinal velocity contours for the configuration of the conventional NACA inlet, case N1A-1. This figure allows verifying that the boundary layer thickness upstream of the NACA inlet is about 50 mm at the beginning of the ramp of the NACA intake. Also, it is clear that the inlet ingests mostly low energy flow.

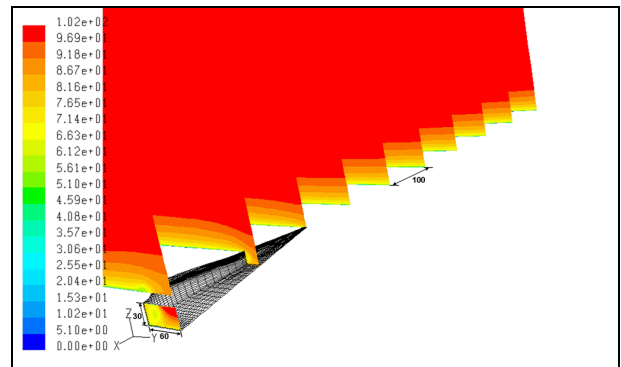


Fig. 6. Longitudinal velocity (m/s) – Case N1A-1 (dimensions in mm).

Fig. 7 shows the distribution of the pressure coefficient along the throat plane of the NACA inlet. It is important to analyze the behavior of the pressure coefficient in this region because the main performance parameter of the NACA inlet, the ram recovery ratio, is defined as the ratio between the dynamic pressure on the throat plane of the NACA inlet and the dynamic pressure of the freestream flow. In this figure the high level of flow distortion originated by the vortex formed above the divergent ramp walls can be clearly seen.

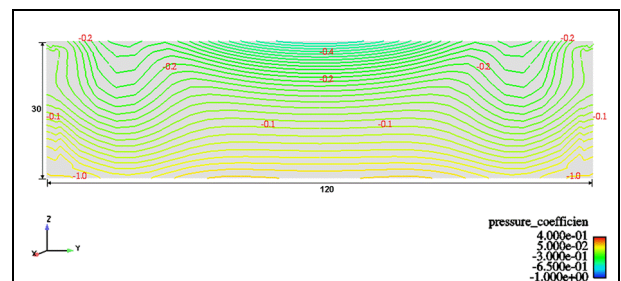


Fig. 7. Pressure coefficient – Case N1A-1, throat plane of the NACA inlet (dimensions in mm).

As mentioned in section 1, the design criteria of the NACA inlets were established during the 1940's and 50's from several experimental works performed in that time, and whose results were later grouped in the ESDU 86002 [11]. The ESDU 86002 is the main tool used to design submerged inlets until today. The design is mainly based on parameters such as ram recovery ratio, mass flow rate or mass flow ratio, drag, inlet geometry and boundary layer thickness.

Since experimental results are not available to validate the numerical results obtained in this

work, design data obtained from ESDU will be used as a reference to select the more appropriate turbulence model to simulate the flow in the NACA intake. Thus, Fig. 8 shows curves of ram recovery ratio, for the results obtained from the ESDU 86002, and from numerical simulations performed using as turbulence model both the Spalart-Allmaras and the k-ε Realizable turbulence model.

In Fig. 8 it is possible to verify that the numerical simulations underestimate the values of the ram recovery ratio of the NACA inlet. In this figure one can observe that the performance trends computed with both turbulence models are quite similar, even if the semi-empirical figures computed from ESDU always exhibit higher values. Considering that the computed values of ram recovery ratio using the Spalart-Allmaras turbulence model showed the smallest discrepancies, about 10%, when compared to the design data obtained from ESDU, and that this turbulence model was specifically developed for aerodynamical applications, it was decided to use only this model on the simulations performed in this work.

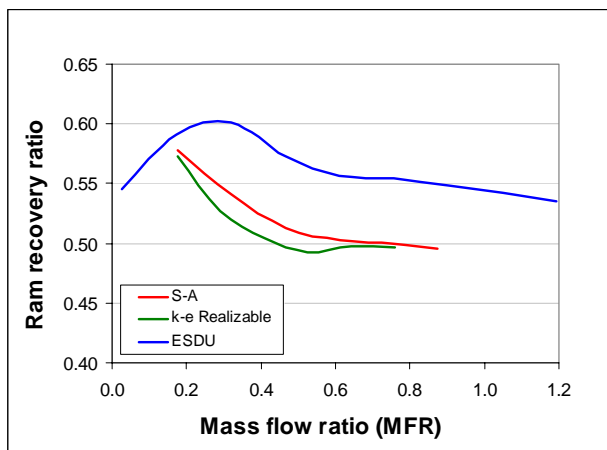


Fig. 8. Characteristic curve of ram recovery ratio of the conventional NACA intake.

3.2 NACA inlet with the freely standing vortex generator

The influence of the use of the delta wing vortex generator upon the development of the boundary layer upstream of the NACA inlet and, consequently, on the performance

parameters of this type of intakes, is analyzed using the same plots used to describe the flow structure in the case of the conventional NACA intake.

Fig. 9 shows cross sections, in transversal planes to the external flow direction, of the longitudinal velocity contours for the basic configuration of NACA inlet with vortex generator, called NGVA. In this figure, it is possible to see that the vortices generated by the delta wing vortex generator lead to a considerable reduction of the boundary layer thickness upstream to the air intake. This substantial reduction takes place mainly at the central region of the flat plate. One immediate consequence of the reduction of the boundary layer thickness is the larger amount of external air ingested by the NACA intake, which leads to increases of the ram recovery ratio and the mass flow rate, such as will be demonstrated later.

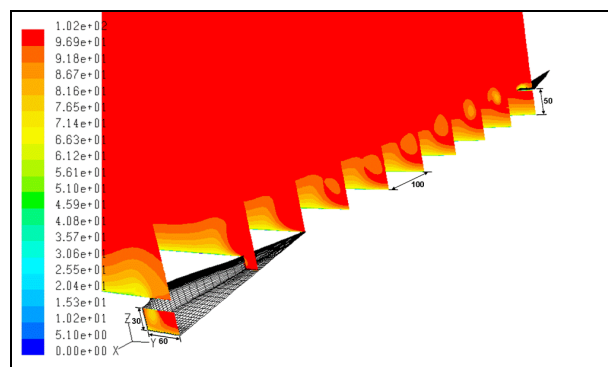


Fig. 9. Longitudinal velocity (m/s) – Case NGVA (dimensions in mm).

The pressure coefficient distribution along the throat plane of the NACA inlet for this configuration (NGVA) is shown in Fig. 10. Comparing this figure with Fig. 7, corresponding to the case N1A-1, it is possible to verify that the presence of the vortex generator produces a flow which is more uniform at the throat of the NACA intake. This decrease in flow distortion is also accompanied by an increase of the performance parameters of the NACA intake, as will be seen further on.

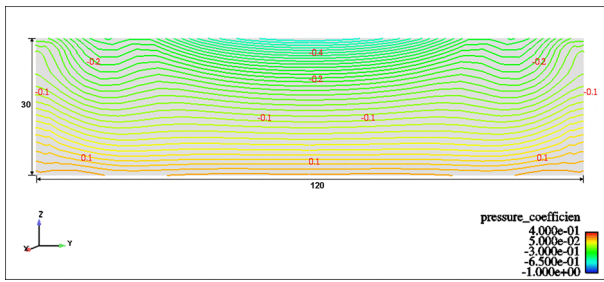


Fig. 10. Pressure coefficient – Case NGVA, throat plane of the NACA inlet (dimensions in mm).

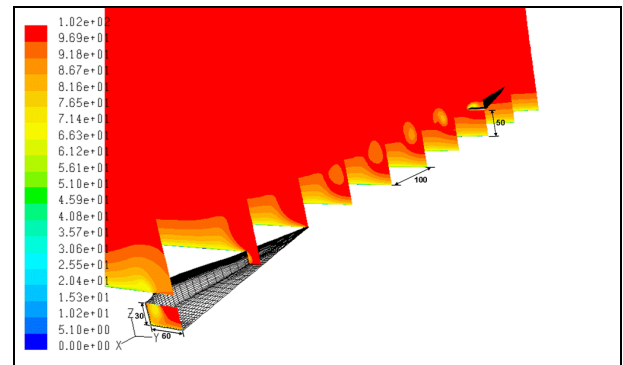


Fig. 11. Longitudinal velocity (m/s) – Case NGVB (dimensions in mm).

3.3 Influence of the horizontal position of the vortex generator

The first parametric variation of the vortex generator geometry studied is the horizontal position of the vortex generator relative to the NACA intake. Two configurations, cases NGVB and NGVC, corresponding to the trailing edge of the vortex generator positioned at a horizontal distance from the ramp beginning of 500 and 300 mm, respectively, were analyzed. These configurations were obtained from variations of the basic configuration of NACA inlet with vortex generator, case NGVA.

Fig. 11 and Fig. 12 show cross sections, in transversal planes to the external flow direction, of the longitudinal velocity contours for the configurations NGVB and NGVC, respectively. In these figures it is possible to verify that the presence of the vortex generator still reduces the boundary layer thickness, essentially at the central region of the flat plate. Comparing these figures with Fig. 9, case NGVA, it is observed that the reduction of the boundary layer thickness is greater in the configuration corresponding to the farthest position of the vortex generator, case NGVA, and that, even if the thickness increases as the vortex generator is placed closer to the NACA intake, it still remains much smaller than in the baseline case N1A-1.

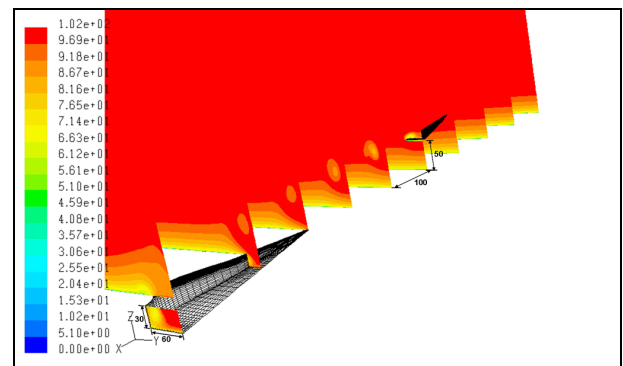


Fig. 12. Longitudinal velocity (m/s) – Case NGVC (dimensions in mm).

The influence of the horizontal position of the vortex generator upon the distribution of the pressure coefficient on the throat plane of the NACA inlet is shown in Fig. 13 and Fig. 14, for the cases NGVB and NGVC, respectively. These figures allow verifying that the reduction of the boundary layer thickness, observed in Fig. 11 and Fig. 12, is accompanied by a decrease of the flow distortion on the throat plane of the NACA intake. Comparing these figures with the Fig. 10, case NGVA, it is possible to note that the level of the flow distortion increases as the vortex generator is placed closer to the NACA intake.

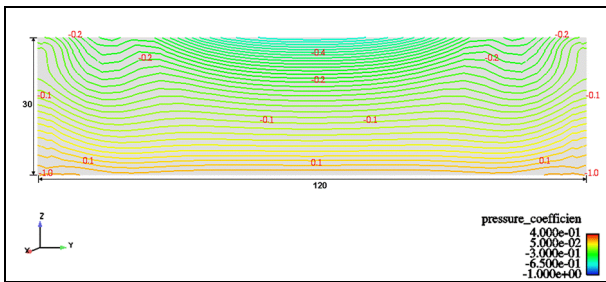


Fig. 13. Pressure coefficient – Case NGVB, throat plane of the NACA inlet (dimensions in mm).

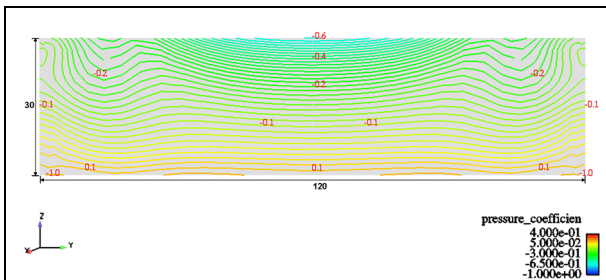


Fig. 14. Pressure coefficient – Case NGVC, throat plane of the NACA inlet (dimensions in mm).

3.4 Influence of the angle of attack (α) of the vortex generator

A parametric variation of the angle of attack (α) of the vortex generator is now presented. Two configurations, cases NGVA-25 and NGVA-35, corresponding to an angle of attack of the vortex generator of 25° and 35° , respectively, were analyzed. Note that these configurations were also obtained from variations of the basic configuration of NACA inlet with vortex generator, case NGVA.

Fig. 15 and Fig. 16 show cross sections, in the same transversal planes to the external flow direction, of the longitudinal velocity contours for the configurations NGVA-25 and NGVA-35, respectively. A comparison of these figures with Fig. 9, case NGVA, shows that the boundary layer development upstream of the NACA inlet and downstream of the vortex generator is certainly influenced by the increase of the angle of attack of the vortex generator. Fig. 15 and Fig. 16 also show that a stronger interaction between the counter rotating vortex downstream the vortex generator occurs as the angle of attack of the vortex generator is increased. This may be responsible by the

observed decrease in performance which goes with the increase in the boundary layer thickness.

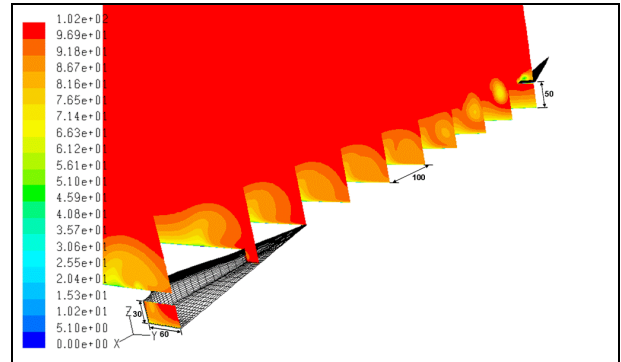


Fig. 15. Longitudinal velocity (m/s) – Case NGVA-25 (dimensions in mm).

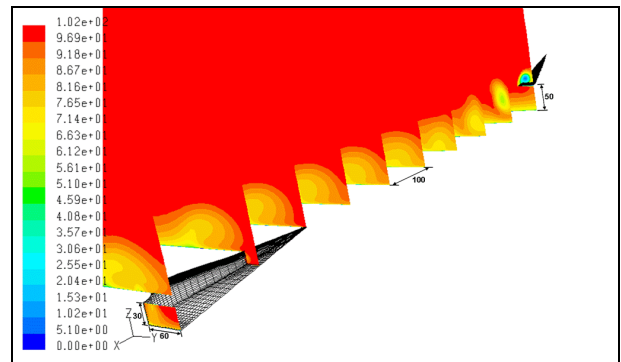


Fig. 16. Longitudinal velocity (m/s) – Case NGVA-35 (dimensions in mm).

The influence of the angle of attack of the vortex generator on the pressure coefficient distribution along the throat plane of the NACA inlet is shown in Fig. 17 and Fig. 18, corresponding to the cases NGVA-25 and NGVA-35, respectively. When these figures are compared to Fig. 10, case NGVA, one can verify that the increase of the angle of attack of the vortex generator originates, first, a decrease and, then, an increase of the flow distortion along the throat plane of the NACA inlet. This deterioration of the flow uniformity on the throat, observed for high values of the angle of attack of the vortex generator, seems to be associated with the strong interaction between the counter rotating vortex pair downstream the vortex generator, which was observed in Fig. 15 and Fig. 16.

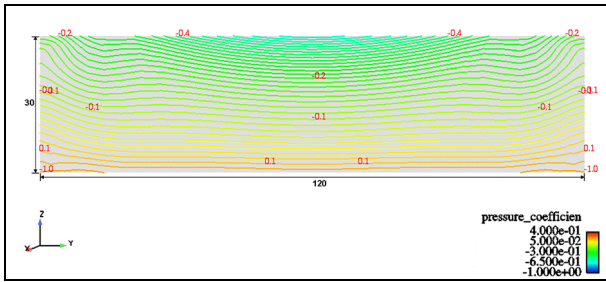


Fig. 17. Pressure coefficient – Case NGVA-25, throat plane of the NACA inlet (dimensions in mm).

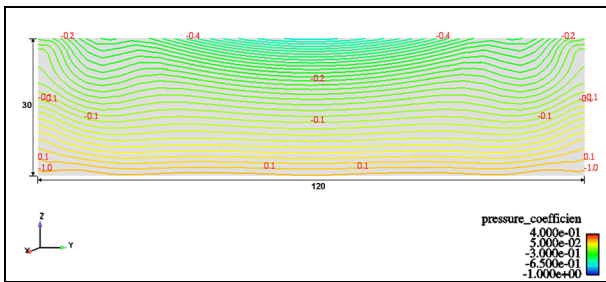


Fig. 18. Pressure coefficient – Case NGVA-35, throat plane of the NACA inlet (dimensions in mm).

3.5 Influence of the area (A) of the vortex generator

The last variation of the vortex generator geometry studied is the area (A) of the vortex generator. Two configurations, cases NGVA-1.5A and NGVA-2.0A, corresponding to increases of 50% and 100% of the area of the vortex generator, respectively, were analyzed. In these configurations, which were obtained from variations of the basic configuration of NACA inlet with vortex generator, case NGVA, the aspect ratio of the vortex generator, i.e., 1.61, remained constant.

Fig. 19 and Fig. 20 show cross sections, in the same transversal planes to the external flow direction, of the longitudinal velocity contours for the configurations NGVA-1.5A and NGVA-2.0A, respectively. Comparisons of these figures with Fig. 9, case NGVA, allow noticing that the increase of the area of the vortex generator increases the transversal extension affected by the flow issued from the vortex generator. As a consequence, upstream of the NACA inlet, the width of the region of destruction of the boundary layer increases in about 50%, when are compared the

configurations NGVA, Fig. 9, and NGVA-2.0A, Fig. 20. However, a central region between the NACA inlet and the vortex generator is practically not affected by the increase of the area of the vortex generator.

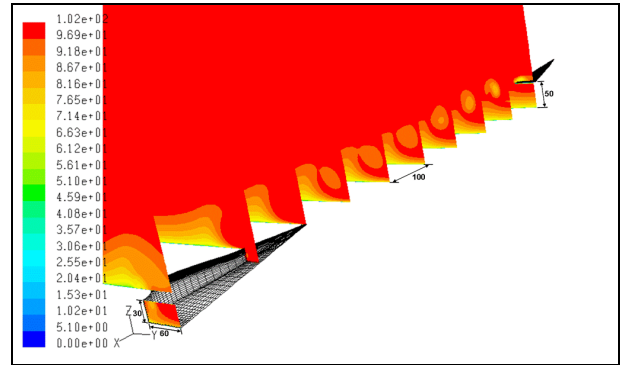


Fig. 19. Longitudinal velocity (m/s) – Case NGVA-1.5A (dimensions in mm).

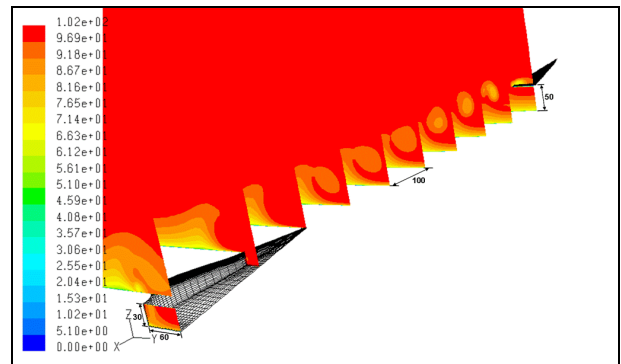


Fig. 20. Longitudinal velocity (m/s) – Case NGVA-2.0A (dimensions in mm).

The influence of the increase of the area of the vortex generator on the pressure coefficient distribution along the throat plane of the NACA inlet is shown in Fig. 21 and Fig. 22, corresponding to the cases NGVA-1.5A and NGVA-2.0A, respectively. A comparison of these figures with Fig. 10, case NGVA, allows verifying that the increase of the area of the vortex generator produces a flow which is progressively more uniform on the throat plane of the NACA intake. This decrease on the level of flow distortion is believed to be related to the increase of the transversal extension of the destruction region of the boundary layer, upstream of the NACA inlet, which was observed in Fig. 19 and Fig. 20.

NUMERICAL STUDY OF THE PERFORMANCE IMPROVEMENT OF SUBMERGED AIR INTAKES USING VORTEX GENERATORS

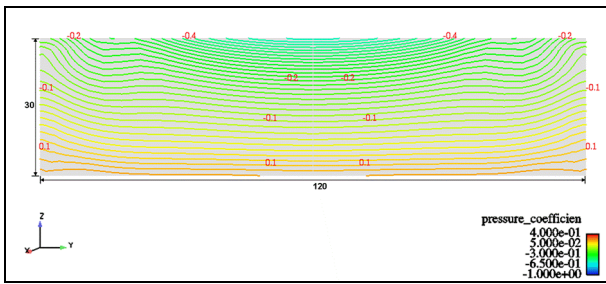


Fig. 21. Pressure coefficient – Case NGVA-1.5A, throat plane of the NACA inlet (dimensions in mm).

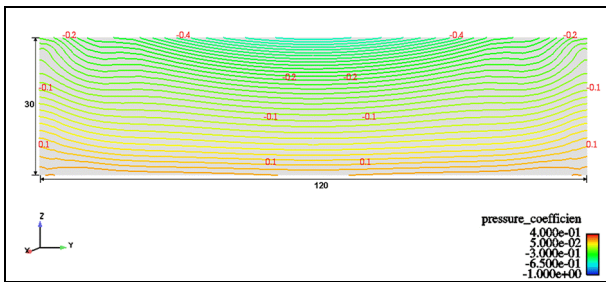


Fig. 22. Pressure coefficient – Case NGVA-2.0A, throat plane of the NACA inlet (dimensions in mm).

3.6 Performance parameters

In this section, the quantitative results, which illustrate the influence of the use of the delta wing vortex generator on the main performance parameters of the NACA inlet, i.e., ram recovery ratio, mass flow rate or mass flow ratio and drag coefficient, are presented.

Table 3 shows the values of the performance parameters for the conventional NACA intake, called N1A-1, and for all the

configurations of NACA intake with vortex generator studied. It is important to emphasize that the values of ram drag, shown in this table, were computed from equations 3.18 and 6.1 of the ESDU 86002 [11]. The friction drag was calculated as the integral wall shear stress of the NACA inlet. Neither the flat plate nor the duct was considered for this drag calculation. The mass flow rate was obtained directly from *Fluent* by integration at the duct exit section of the NACA intake. In this table, the percentage increases related to the values of the parameters corresponding to the conventional NACA inlet are indicated in the parentheses.

The results shown in Table 3 indicate that all the configurations of NACA inlet with the freely standing vortex generator studied exhibit significant improvements for the computed values of mass flow rate and ram recovery ratio. The largest increases in these performance parameters are obtained for the vortex generators of increased area.

Regarding the variations of the horizontal position of the vortex generator, the best results are obtained for the farthest position of the vortex generator, case NGVA. As the vortex generator is displaced downstream, the gains decrease, but remain significant. Regarding the increases of the angle of attack of the vortex generator, it is important to note that significant improvement is achieved in the figures of the mass flow rate and ram recovery ratio for angle of attack of vortex generator of 25°. However,

Table 3. Performance parameters of the NACA inlet with and without the delta wing vortex generator.

Parameters	N1A-1	NGVA	NGVB	NGVC	NGVA-25	NGVA-35	NGVA-1,5A	NGVA-2,0A
Ram-recovery ratio	0.513	0.741 (44.4 %)	0.713 (39 %)	0.647 (26.2 %)	0.754 (46.9 %)	0.717 (39.7 %)	0.79 (54 %)	0.808 (57.5 %)
Mass-flow rate (kg/s)	0.260	0.302 (16 %)	0.297 (14.2 %)	0.294 (12.9 %)	0.304 (16.9 %)	0.298 (14.6 %)	0.31 (19.3 %)	0.313 (20.5 %)
Mass-flow ratio - MFR	0.76	0.88 (16 %)	0.87 (14.2 %)	0.86 (12.9 %)	0.89 (16.9 %)	0.87 (14.6 %)	0.91 (19.3 %)	0.91 (20.5 %)
Total drag - (N)	18.60	32.43 (74.4 %)	31.48 (69.3 %)	29.08 (56.3 %)	36.65 (97 %)	40.4 (117.2 %)	34.5 (85.5 %)	36.02 (93.6 %)
Ram drag - (N)	18.13	31.69 (74.7 %)	30.77 (69.7 %)	28.41 (56.7 %)	35.93 (98.1 %)	39.71 (119 %)	33.69 (85.8 %)	35.15 (93.8 %)
NACA	18.13	29.68 (63.7 %)	28.79 (58.8 %)	26.43 (45.7 %)	30.01 (65.5 %)	29.32 (61.7 %)	30.59 (68.7 %)	30.9 (70.4 %)
VG	0.00	2.01	1.98	1.98	5.92	10.38	3.10	4.25
Support	0.00	0.00	0.00	0.00	0.00	0.00	0.00	0.00
Friction drag - (N)	0.47	0.74 (60 %)	0.71 (53.3 %)	0.67 (43.4 %)	0.72 (54.2 %)	0.69 (47.9 %)	0.81 (73.4 %)	0.87 (86.5 %)
NACA	0.47	0.59 (26.5 %)	0.56 (19.8 %)	0.51 (9.5 %)	0.57 (23.5 %)	0.56 (19.8 %)	0.6 (28 %)	0.6 (29.4 %)
VG	0.00	0.16	0.16	0.16	0.14	0.13	0.21	0.27
Support	0.00	0.00	0.00	0.00	0.00	0.00	0.00	0.00
Drag coefficient	1.06	1.86 (74.4 %)	1.8 (69.2 %)	1.66 (56.3 %)	2.1 (97 %)	2.31 (117.2 %)	1.97 (85.5 %)	2.06 (93.6 %)

when this angle is increased to 35° , there is a reduction of performance. This behavior indicates that there is an optimum value for the angle of attack of the vortex generator.

Considering that the increases of the area of the vortex generator originate a penalty, in terms of drag coefficient, lower, in both cases, than in the best case of the variation of the angle of attack, 25° , it may be concluded that increasing the area of the vortex generator is the best route to improving the performance of the NACA intakes.

Besides, in Table 3 it can be seen that the values of drag coefficient also exhibit a significant increase for all the configurations of NACA inlet with vortex generator. This is a direct consequence of both the increase of mass flow rate and the decrease of the boundary layer thickness. In the cases related to the increase of angle of attack of the vortex generator, the greater frontal area of the vortex generator also contributes to the increase of the drag coefficient. Even so, the drag contribution due to the vortex generator is only about 25% of the total drag of the ensemble in the case of the highest angle of attack of the vortex generator, and about 10% in the case that the area of the vortex generator is increased in 100%.

4 Conclusions and perspectives

In this work, the flow structure on the NACA intake and the influence of the vortices generated by a delta wing vortex generator upon the boundary layer development upstream of the NACA inlet was studied.

The computational results show that the presence of the freely standing vortex generator, in all the configurations studied, is responsible for considerable reductions of the boundary layer thickness and, consequently, significant improvements of the performance parameters of the NACA inlet. The improvements, relative to the conventional NACA intake, in terms of ram recovery ratio and mass flow rate, are of up to 57.5% and 20.5%, respectively. The contribution of the drag induced by the presence of the vortex generator on the total drag of the

ensemble is small, about 10%. However, the total drag coefficient presents a considerable increase, of the order of 90%, which is a direct consequence of both the increase of mass flow rate and the decrease of the boundary layer thickness.

Future work should involve the study of other parametric variations, including combinations of already studied, in order to optimize the vortex generator geometry. Also, installation effects should be examined by the inclusion of supporting masts. Finally, experiments are required in order to validate the results obtained in this numerical study.

5 References

- [1] Nogueira de Faria W and Oliveira G L. Análise de entradas de ar tipo NACA com gerador de vórtices. *9th Brazilian Congress of Thermal Engineering and Sciences - ENCIT 2002*, Caxambu - MG - Brazil, CIT02-0758, 2002.
- [2] Devine R J, Watterson J K, Cooper R K and Richardson J. An investigation into improving the performance of low speed auxiliary air inlets using vortex generators. *20th AIAA Applied Aerodynamics Conference*, St. Louis - Missouri, AIAA 2002-3264, 2002.
- [3] Hall C F and Frank J L. Ram-recovery characteristics of NACA submerged inlets at high subsonic speeds. I-inlets forward of the wing leading edge. *NACA RM A8I29*, 1948.
- [4] Delany N K. An investigation of submerged air inlets on a $1/4$ -scale model of a fighter-type airplane. *NACA RM A8A20*, 1948.
- [5] Taskinoglu E S, Jovanovic V, Doyle D K and Elliot G S. Multi-objective design optimization and experimental measurements for a submerged inlet. *42nd AIAA Aerospace Sciences Meeting and Exhibit*, Reno - NV, AIAA 2004-25, 2004.
- [6] Gorton S A, Owens L R, Jenkins L N, Allan B G and Schuster E P. Active flow control on a boundary-layer ingesting inlet. *42nd AIAA Aerospace Sciences Meeting and Exhibit*, Reno - NV, AIAA 2004-1203, 2004.
- [7] Mossman E A and Randall L M. An experimental investigation of the design variables for NACA submerged duct entrances. *NACA RM A7I30*, 1948.
- [8] ANSYS, Inc. *ANSYS ICEM CFD*. <<http://www.ansys.com/products/icemcf.asp>>.
- [9] Fluent, Inc. *FLUENT Flow Modeling Software*. <<http://www.fluent.com/software/fluent/index.htm>>.

- [10] Spalart P R and Allmaras S R. A one-equation turbulence model for aerodynamic flows. *La Recherche Aéronautique*, No. 1, 1994, pp. 5-21.
- [11] Engineering Sciences Data Unit, ESDU. *Drag and pressure recovery characteristics of auxiliary air inlets at subsonic speeds*. Item N° 86002 with amendments A and B, London 1996.

6 Acknowledgments

The authors wish to thank Embraer, CNPq and Fapesp for the support provided for this work. During this work Luís Fernando Figueira da Silva was on leave from the Laboratoire de Combustion et de Détonique (Centre National de la Recherche Scientifique, France). Miss Leticia Hime participated at the vortex generator definition. Mesh generation was performed by Mr. Rodrigo Ferraz, from ESSS (Engineering Simulation and Scientific Software Ltda.).